Bivariate statistics of wind farm support vessel motions while docking

Oleg Gaidai[1*)], Xiaosen Xu[2)], Arvid Naess[3)], Yong Cheng[1)], Renchuan Ye[1)], Junlei Wang[4)]

[1)] Jiangsu University of Science and Technology, Zhenjiang, China
[2)] Florida Institute of Technology, USA
[3)] Norwegian University of Science and Technology, Norway
[4)] School of Mechanical and Power Engineering, Zhengzhou University, China

1 Abstract

Robust prediction of extreme motions during wind farm support vessel (WFSV) operation is an important safety concern. In particular, it is important to study safety of operation in random sea conditions during WFSV docking against the wind tower, while workers are able to get on to the tower. Docking is performed by thrusting the vessel fender against the wind tower (the alternative docking maneuver by hinging is not studied here). In this paper, the finite element software AQWA has been used to analyze the vessel response due to hydrodynamic wave loads, acting on a specific maintenance ship under actual sea conditions. Excessive motions may occur during certain sea conditions, posing a risk to the crew transfer operation. The authors have primarily focused on the statistical analysis rather than the dynamics of the problem.

This paper presents a novel method for estimating bivariate statistics, based on Monte Carlo simulations (or measurements if available). The bivariate average conditional exceedance rate (ACER2D) method is briefly outlined. The ACER2D method offers an accurate estimation of bivariate statistics, utilizing the available data efficiently. Two dimensional probability contours, corresponding to large return periods, are obtained by the ACER2D method. Based on the overall performance of the presented method, it is seen that the ACER2D method provides an efficient and accurate prediction of extreme return period contours.

The described approach may serve as a useful tool for vessel design, facilitating optimization of boat parameters in order to minimize excessive vessel motions.

Keywords

Wind farm support vessel (WFSV); docking; Monte Carlo; bivariate distribution; offshore wind turbine; wind energy.

2 Introduction

The offshore renewable wind energy market is expected to have a dramatic growth in the next decades. Operational costs and safety issues related to wind farm maintenance are among the most crucial issues for the renewable energy sector. For an onshore wind farm, the maintenance tasks can be carried out almost at any time when the weather conditions are not extreme. On the other hand, for an offshore wind farm (OWF) operation, a number of issues like transportation of maintenance personnel, equipment, spare parts, and access to the wind turbines from service vessels are restricted by sea conditions. Down time of wind turbines due to waiting for weather windows is one of the major contributors to the loss of electricity production and hence income. Innovative vessel and access concepts can help to

[*)] Corresponding author: Oleg Gaidai, tel. +8618852803218; email: o_gaidai@just.edu.cn

reduce the weather restrictions on the access operation and therefore decrease the downtime for offshore wind turbines. The latter implies that certain savings in costs and increase in operational safety can be obtained by optimizing vessel characteristics, especially on the design stage.
An accurate modeling of the WFSV extreme motions during docking against the wind tower should be conducted in order to evaluate operational risks. Relatively few studies have been done in the latter direction, see e.g. Bondarenko(2015); Wu (2014) for the docking operation numerical analysis of the WFSV with a simple fender. See also Zhang et al . (2014a) for a study of ooperation modelling of a WFSV using stochastic activity networks.

A certain amount of research work has been done to study the motions of WFSV in waves, see e.g. Wu (2014); Zhang et al. (2014a); Zhang et al. (2014b); Naess and Moan (2013); Price and Bishop (1974); Sandvik (2010); Phillips et al. (2014); Phillips et al. (2015) for the WFSV docking operation with a fender system. Analyzing complex vessel motions during step-across-fender transfer are of importance for safety of operations, see Phillips et al. (2014); Phillips et al. (2015). Statistics of extreme motions is a key issue for the safety and reliability analysis during offshore operations; see Bondarenko(2015); Naess and Moan (2013); Price and Bishop (1974) for the basics of the probabilistic theory for ships and offshore structures.
It can be concluded from a study of the existing literature that there is no preferred methodology for prediction of the WFSV extreme motion statistics. Vessel heave and pitch are among of the most critical vessel motion types, having an important effect on the transfer safety during docking operation. This paper studies extreme value statistics of WFSV combined heave and pitch motions, during docking against a wind tower in random sea conditions.

The aim of this paper is to develop a simple and general Monte Carlo (MC) based method, which is able to tackle all nonlinear effects without simplifications, except for those inherent in the hydrodynamic model itself. This goal has been achieved by combining standard MC simulations with a CPU time-saving extrapolation scheme Naess and Karpa (2015); Karpa and Naess (2015); Gaidai et al. (2016).
As opposed to univariate statistical methods, the ACER2D method takes into account bivariate correlation, which may reflect important coupling effects. Due to only partial correlation between the vessel heave and pitch angles, application of the multivariate, or bivariate in the simplest case, extreme value theory is of practical interest. The bivariate ACER2D method is not the only approach that serves estimating bivariate statistics, see as example Heffernan and Tawn (2004); Ewans (2014) for the IFORM (inverse first order reliability method), or SORM (second order reliability method), see e.g. Zhao and Ono (1999). An advantage of the ACER2D method is that it does not rely on asymptotic assumptions and do not exclude non-linearities.

3 Wave statistics

Satellite based global wave statistics was used to obtain the wave scatter diagram in the Bohai bay area, where the wind farm is located. Specifically, commercial Global Wave Statistics Online data http://www.globalwavestatisticsonline.com/ was purchased. Table 1 presents directional probabilities of wind and waves in Bohai bay http://www.globalwavestatisticsonline.com/, Lv et al. (2014) averaged over the whole year (seasonal variations are averaged). Fig. 1 presents annually averaged spatial distributions of wave height in Bohai bay Lv et al. (2014) ; Zhang et al. (2018).

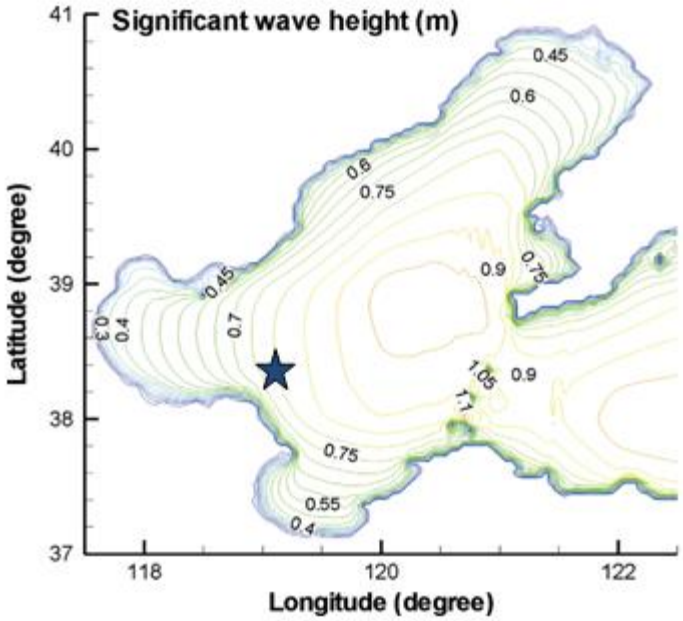

Fig. 1 Annually averaged spatial distribution of wave height in Bohai Sea, Lv et al. (2014). Star indicates WFSV location.

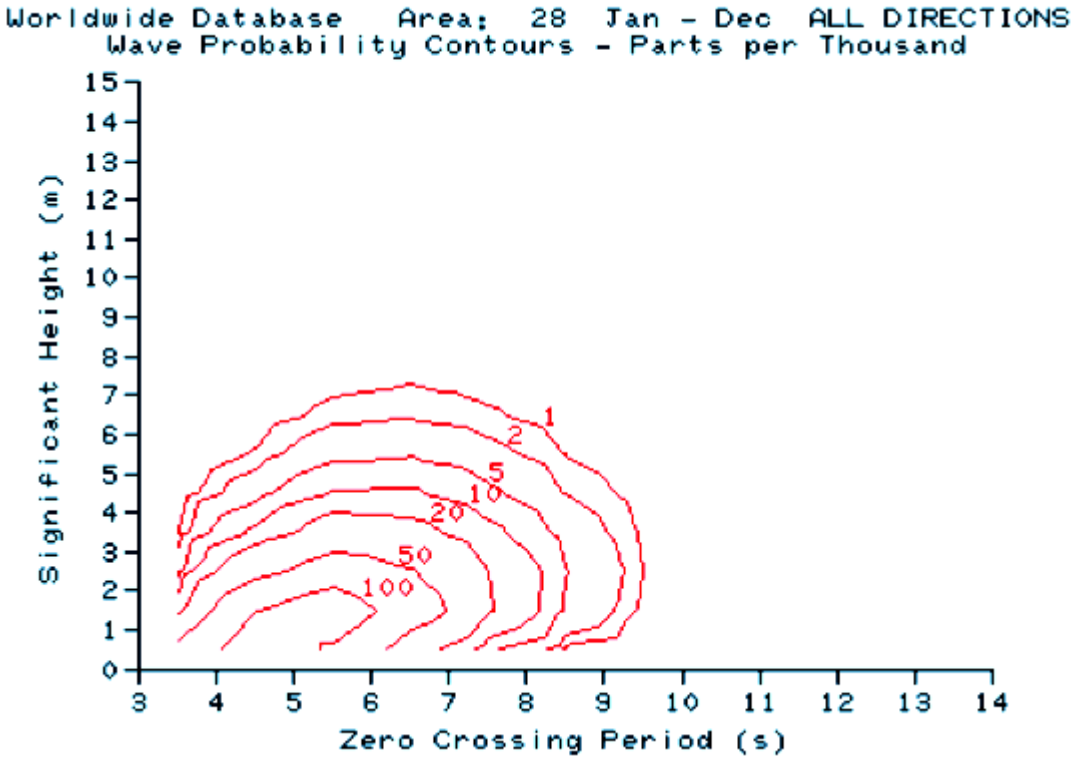

Fig. 2 Environmental contour lines for Bohai bay area from http://www.globalwavestatisticsonline.com/. Contour numbers: fare parts per thousand.

Fig. 2 presents environmental contour lines for the Bohai bay area, averaged annually and averaged over all eight wave directions. Due to the limitation of WFSV operating in the sea with significant wave height H_s larger than 1.6 m, sea states with wave height over 1.6 m were removed from the measured sea state dataset. Thus statistics has been made conditional on the operational safety requirement. Subsequently, an approximate sea state scatter diagram was estimated based on environmental contour lines data from Fig. 2. The modified scatter diagram (once the wave heights larger than 1.6m have been removed) has not been presented in this paper due to its low resolution, justifying it by the fact that the aim of the proposed paper was an illustration of statistical technique, and not

an accurate in situ engineering estimate. The zero crossing period from Fig. 2 is approximately linearly related to the spectral peak wave period T_p, see DNV rule DNV-RP-H103 (2011).

Table 1 Directional probabilities of wind and waves in Bohai bay http://www.globalwavestatisticsonline.com/.

Direction	*All Year*
North-East	14.89 %
East	11.11 %
South-East	10.01 %
South	13.15 %
South-West	7.65 %
West	8.16 %
North-West	14.21 %
North	20.82 %

Fig. 2 presents an environmental contour plot averaged over the eight wave directions, as authors did not want to present eight different directional environmental contour plots. The separate wave statistics per each direction was available from (http://www.globalwavestatisticsonline.com/).

A three hour stationary storm simulation was run for each sea state of each directional sea state (H_s, T_p), approximately estimated based on Fig. 2. For each particular directional storm at a certain significant wave height the total of 8 random sea realizations (random seeds) have been generated, amounting to $T_{tot} = 24$ hours direct Monte Carlo simulation for each sea state, the latter T_{tot} is typical for offshore engineering applications, see e.g. Karpa (2015); Naess et al (2007). As an overview, Fig. 3 presents a flow chart for the methodology applied in this paper. The significant wave height in the simulation ranged from 0.6 m to 1.6 m with the bin size of 0.2 m. First 600 s simulation results have been discarded due to initial transient effects.

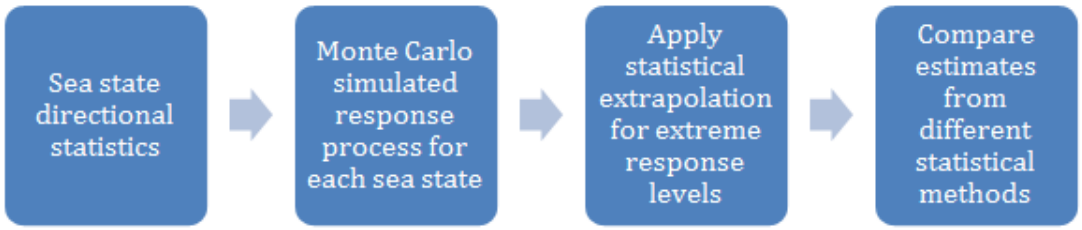

Fig. 3 Flow chart for the described methodology.

The random stationary sea states are specified by a JONSWAP wave spectrum, that is, the one-sided power spectral density (PSD) of the wave elevation $\eta(t)$, denoted by $S_\eta^+(\omega)$, is given as follows $(\omega > 0)$

$$S_\eta^+(\omega) = \frac{\alpha g^2}{\omega^5}\exp\{-\frac{5}{4}(\frac{\omega_p}{\omega})^4 + \ln\gamma\exp[-\frac{1}{2\sigma^2}(\frac{\omega}{\omega_p}-1)^2]\}$$

with $g = 9.81$ m/s^2, ω_p denoting the peak frequency in rad/s; and α, γ and σ being parameters related to the spectral shape; $\sigma = 0.07$ when $\omega \le \omega_p$, $\sigma = 0.09$ when $\omega > \omega_p$. For the Bohai bay, the parameter γ is chosen to be equal to 3.3, see Wang et al. (2012); the parameter α is determined from the following empirical relationship $\alpha = 5.06(\frac{H_s}{T_p^2})^2(1-0.287\ln\gamma)$, see DNV rules DNV-RP-C205 (2010); DNV-RP-H103 (2011). H_s is the significant wave height, and $T_p = 2\pi/\omega_p$ is the spectral peak wave period.

4 Modelling of vessel motions during docking in waves, using AQWA

AQWA software has been developed by ANSYS Inc. It is an efficient tool for simulating nonlinear wave loading on

both floating and fixed rigid bodies, as well as nonlinear vessel responses, see AQWA users manual (2013). The latter is done by employing three-dimensional radiation/diffraction theory in regular waves in the frequency domain. To account for coupling between floating body dynamics and structural response, the AQWA software employs specific modules such as AQWA (diffraction model), AQWA WAVE (linking program), and ANSYS (structural finite element analysis).

Unidirectional or multidirectional second order drift forces can be evaluated by the far-field, near field solution, or full quadratic transfer function (QTF) matrix. Free floating hydrostatic and hydrodynamic analyses in the frequency domain can be performed as well, see AQWA users manual (2013).

The real-time motion of a floating body while operating in regular or irregular waves can be accurately simulated with AQWA, with nonlinear Froude-Krylov and hydrostatic forces being estimated under instantaneous incident wave surface. The real-time motion of a floating body while operating in irregular waves, can be simulated under first- and second-order wave excitations.

Fig. 4 Fender docking operation of the maintenance ship against wind tower.

Fig. 5 on the left corresponds to Fig. 4 and it shows the corresponding AQWA finite element model of the wind turbine tower and maintenance ship during fender docking against wind tower. As noted above, this paper considers the vessel thrusts with fender against the wind tower, as opposed to the vessel hinging to wind tower.

Table 2 Some WFSV vessel parameters.

Parameter	*Value*	*Unit*
Length between perpendiculars	18.0	m
Breadth	6.5	m
Draft	1.3	m
Displacement tonnage	42.0	tones
Longitudinal center of gravity	8.0	m
Vertical center of gravity	2.5	m

Table 2 presents some basic WFSV vessel parameters. Both 1st and 2nd order forces are computed in AQWA by utilizing linear transfer function (LTF) and quadratic transfer function (QTF).

Fig. 5 on the right presents a top view of the fender during docking. Several different access/docking devices are typically employed between a service vessel and a wind turbine. In this paper the simplest type is modelled, namely a fender made of rubber or other materials. The bollard push force from the propulsion system keeps the ship bow attached to the wind turbine tower (foundation) while the personnel access the ladder on the tower from the bow.

The punctual contact or friction force tends to restrict relative translational motions (surge, sway and heave) to almost zero, but does not assure that the relative angular motion (roll, pitch and yaw) between the two elements of the contact be zero. This is the way the roll motion of the maintenance ship is different to that of the wind turbine tower. The friction moment was neglected in the roll motion calculation. The fender friction force F_f on the contacting surface was given by $F_f = \mu T$, where μ is the friction coefficient, and T is the normal compression reaction force.

In this paper the AQWA-Drift time-domain simulation approach was adopted to model the vessel motions and the non-linear reaction forces between the fender and the wind turbine tower. The fender damping force F_d was only applied in the direction of the fender compression force. A linear material damping model is adopted in AQWA, namely $F_d = \beta K_f \frac{dL_d}{dt}$, with β being the damping coefficient and K_f being the fender stiffness, and L_d being the distance between the two contacting points of the fender, see AQWA theory manual (2013) for details.

Fig. 6 presents an example of the roll moment QTF in dimensional form, per unit length squared, in the beam sea: difference frequency (left) and sum frequency (right). As expected, the sum frequency QTF has sharp peaks, while the difference frequency QTF, which is responsible for vessel slow motions, is much less 'peaked'.

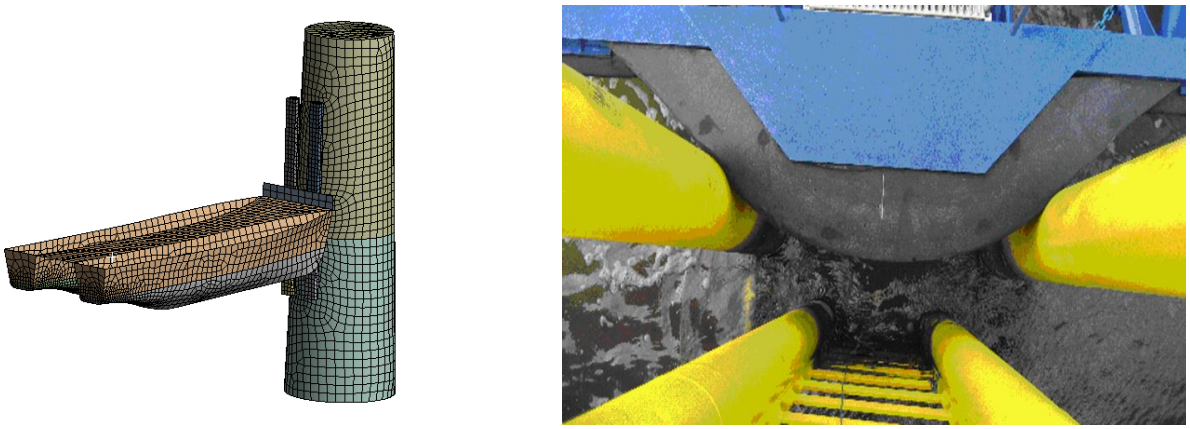

Fig. 5 Coupled panel model of the wind turbine tower and maintenance ship (on the left); a top view of fender during docking (on the right).

The numerical simulation was based on AQWA-Line and AQWA-Drift models are utilized to perform the frequency-domain analysis and the time-domain analysis respectively. Thus AQWA-Line tool was used to generate vessel LFT and QTF transfer functions. Vessel current and wind force coefficients at different incident angles were calculated using commercial ANSYS Fluent software and applied in the AQWA-Drift model, see AQWA theory manual (2013).
The fender and its wind tower interaction force were simulated in the AQWA-Drift (time-domain) model and the diameter of the fender was 0.2m. Bollard push force was put at the aft of the support vessel and its value was set to 80kN. Table 2 presents some basic WFSV vessel parameters.

The size of the mesh was chosen smaller than 1/7 of the shortest wave length; the time step was chosen smaller than 1/10 of the smallest wave period, in accordance with AQWA requirements. The mesh size and time step Δt were chosen in accordance with AQWA convergence criteria, to ensure accuracy of simulated results, particularly vessel motions in waves. For the sake of assuring convergence, time step Δt has been halved for the one selected sea state, and numerical results have been found convergent with original simulation.

Finally, a brief discussion follows regarding numerical modelling of physical phenomena, such as for example ship maneuvering, occurring during docking of the vessel to the platform. Employing a CFD solver to solve Navier-Stokes equations is not unique, but one possible approach to simulate ship motions. For an overview of state-of-the-art of ship motion modeling, see Reed and Beck(2016). However, including all relevant hydrodynamic components, such as e.g. lifting/ maneuvering forces and viscosity effects, was not a practical approach for a long-term simulation, since it would require prohibitively large computational costs. Besides, AQWA is computationally less expensive than, say solving directly the full Navier-Stokes equations. Note that AQWA is based on potential flow theory and it takes non-linear hydrodynamic forces as well as coupled multi-body interaction into consideration. Viscous damping coefficients were added in AQWA in order to compensate for the deficiency of the potential flow theory. Wind and current drag coefficients were also calculated by using ANSYS Fluent and added to AQWA.

The purpose of the maintenance ship is to transfer the personnel and equipment, and the process of transferring usually takes only minutes. Therefore the maneuvering is not of importance in this study, due to short duration of transferring.

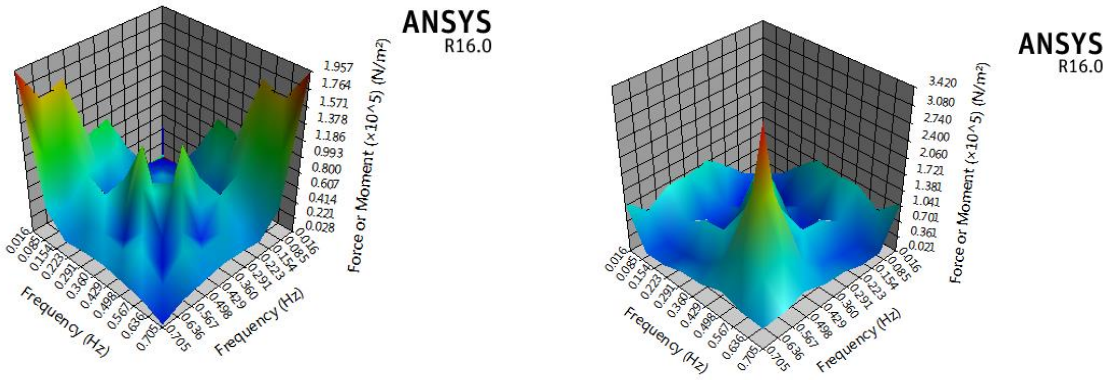

Fig. 6 Example of heave QTF amplitude: difference frequency (left) and sum frequency (right).

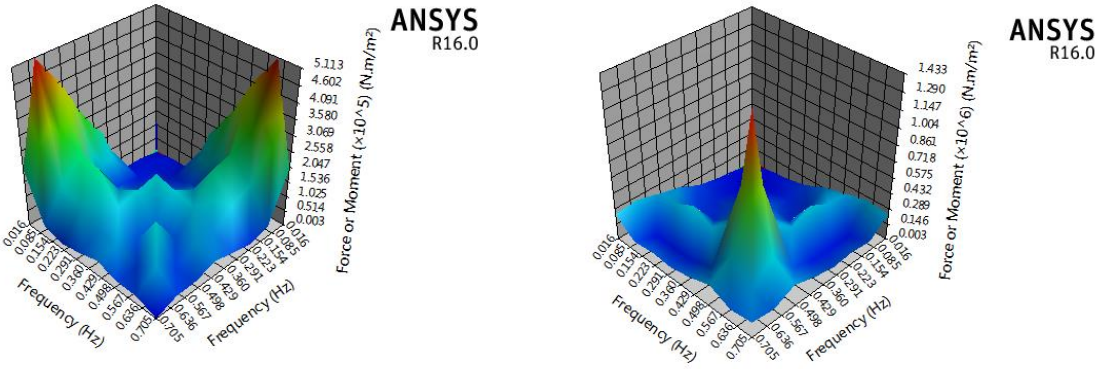

Fig. 7 Example of pitch angle QTF amplitude: difference frequency (left) and sum frequency (right).

Fig. 6 presents an example of the heave QTF (quadratic transfer function) amplitude in the 45 °directional sea, Fig. 7 presents an example of the pitch angle QTF; difference frequency (left) and sum frequency (right). The numerical simulation utilized AQWA-Line and AQWA-Drift models to perform frequency-domain and time-domain analysis respectively. The 1st order and 2nd forces have been computed in AQWA. The numerical simulation was based on AQWA-Line and AQWA-Drift models to perform the frequency-domain analysis and the time-domain analysis, respectively. Thus AQWA-Line FEM tool was used to generate vessel LTF (linear transfer function) and QTF transfer functions. Vessel current and wind force coefficients at different incident angles were calculated in Fluent and applied in the AQWA-Drift model.

The fender along with its wind tower interaction force were simulated in the AQWA-Drift (time-domain) model. The size of the mesh was chosen smaller than 1/7 of the shortest wave length; the time step was chosen smaller than 1/10 of the smallest wave period, in accordance with AQWA requirements. The relevant experimental validation of AQWA numerical results, see Xu et al. (2019a); Xu et al. (2019b) discussing experimental results on the FPSO (floating production storage and offloading unit) vessel, insures that AQWA is a proper and accurate tool to study complex vessel motions. Both WFSV transfer operation and FPSO offloading operation exhibit similar nature of combined wave motions and structural interactions.

5 Statistical approach – the ACER2D method

The Averaged Conditional Exceedance Rate (ACER2D) method has been applied to analyse vessel motion data in order to assess the extreme bivariate heave and pitch statistics. The major advantage of the ACER2D method is that it takes into account the full non-stationary data set, and it allows a pre-asymptotic behaviour, rather than relying on an ad-hoc asymptotic assumption. Note that both the stochastic processes (heave and pitch in this paper) are required to be synchronous in time, which allows an in-depth look into the long term correlation statistics and coupling effects. The brief decription of the bivariate ACER2D method is given in Appendix, for more details see Naess and

241 Karpa (2015); Karpa and Naess (2015); Gaidai et al. (2016).

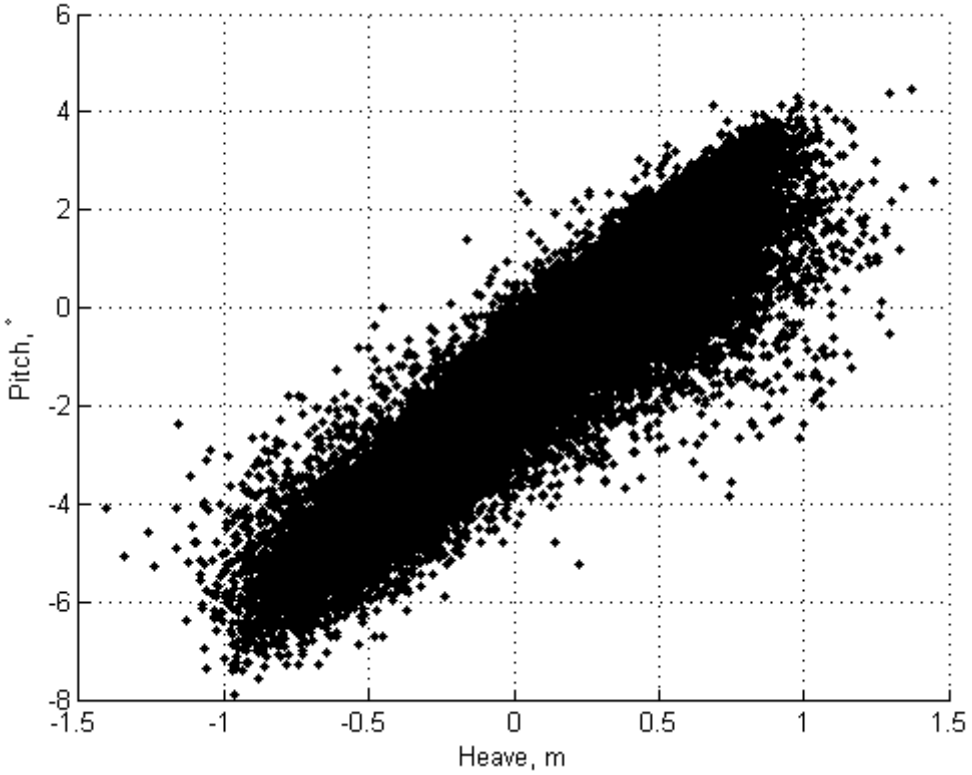

242

243 **Fig. 8 Vessel COG heave (meters) versus synchronous pitch angle (degrees).**

244

245 Fig. 8 illustrates the vessel's center of gravity (COG) heave displacement versus the synchronously recorded pitch
246 angle. This would represent a sample of the long term bivariate distribution of heave and pitch, which clearly
247 displays a significant correlation between the two random variables.

248

249

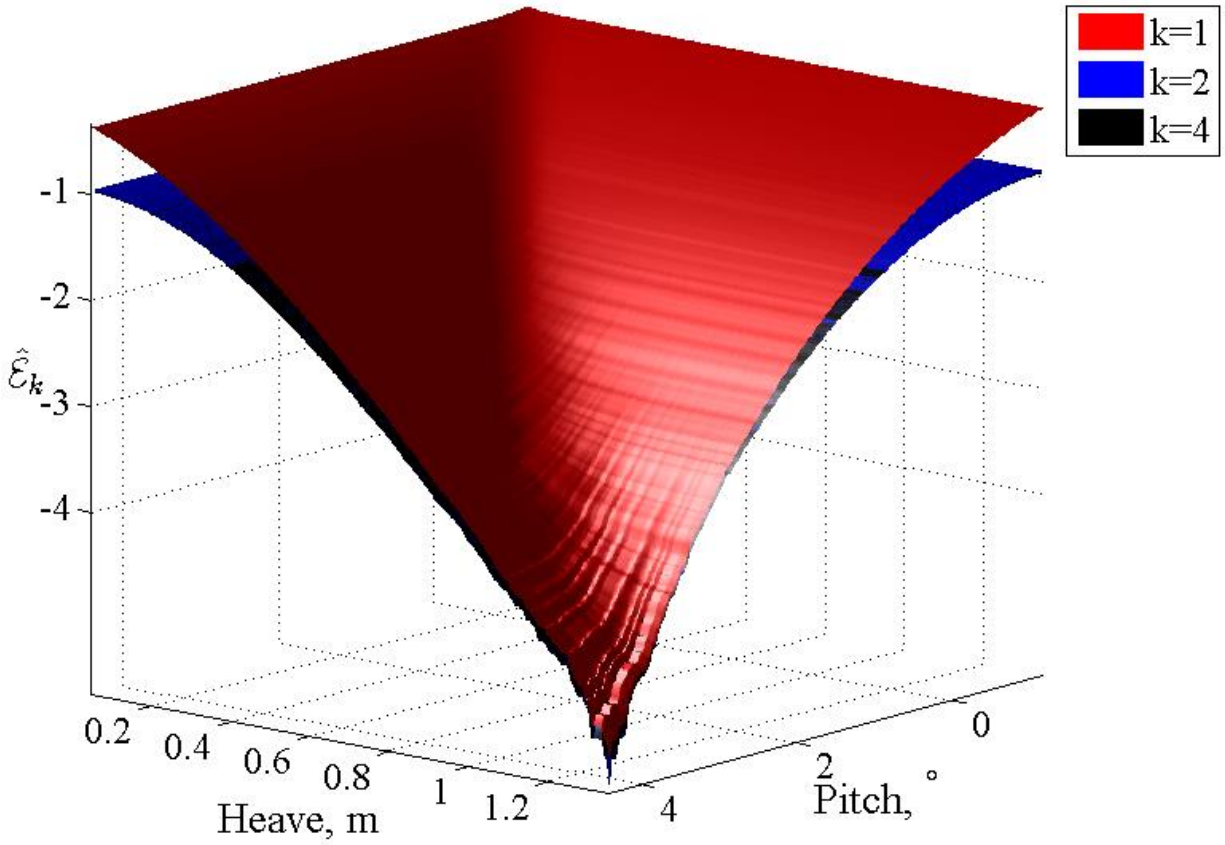

Fig. 9 Comparison between ACER2D surfaces for different degrees of conditioning. $\hat{\mathcal{E}}_k(\xi,\eta)$ functions are plotted on a decimal logarithmic scale; ξ is heave, η is pitch angle.

Fig. 9 presents the empirically estimated bivariate ACER2D functions $\hat{\mathcal{E}}_k(\xi,\eta)$ for different conditioning values of k on a decimal logarithmic scale. $\hat{\mathcal{E}}_k(\xi,\eta)$ with $k=1$ is represented by the upper surface, while the following surfaces that converge in the tail for $k \geq 2$. As it is seen from the Fig. 9, the cross-section of the surfaces at the high level of heave ξ gives the univariate ACER2D functions of the pitch angle η, while the cross-section at a high pitch angle level represents the univariate ACER2D of the heave, respectively. Since the surfaces for $k \geq 2$ have converged in the tail and estimation of $\hat{\mathcal{E}}_2(\xi,\eta)$ is more accurate due more data availabile, one is to choose the function (and thus its surface) with the degree of conditioning $k=2$.

Fig. 10 Left presents contour lines for the optimized Asymmetric logistic (AL) $\mathcal{A}_k(\xi,\eta)$ and optimized Gumbel logistic (GL) $\mathcal{G}_k(\xi,\eta)$ models, optimally fit to the empirical bivariate ACER2D function $\hat{\mathcal{E}}_k(\xi,\eta)$, $k=2$, see Appendix for GL and AL definitions. The negative numbers at the contour lines in Fig. 10 indicate probability levels of $P(\xi,\eta)$ from Eq. (1) in Appendix on a decimal logarithmic scale. Fig. 10 Left shows that the empirical bivariate ACER2D surface $\hat{\mathcal{E}}_2$ captures quite well the high correlation between the data. It is also seen that the optimaized models $\mathcal{G}_2$ and $\mathcal{A}_2$ give smooth complete contours. Note that if the bivariate data would be fully correlated, the contour lines would consist of only horizontal and vertical straight segments. Fig. 10 Left shows quite good agreement between the estimated bivariate ACER2D and the optimized AL and GL surfaces.

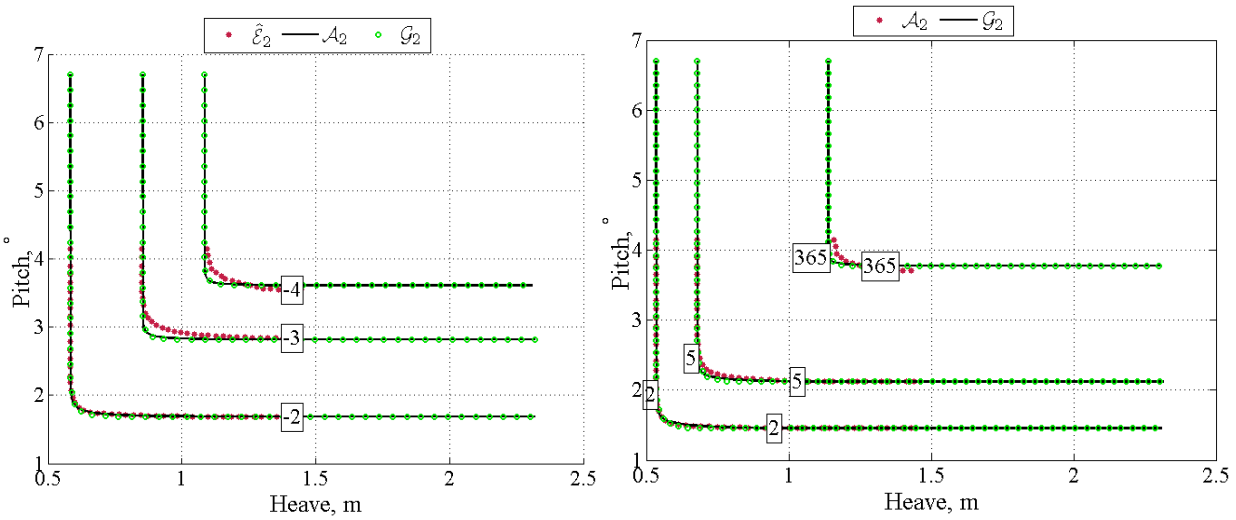

Fig. 10 *Left*: **Contour plot of the empirically estimated $\hat{\mathcal{E}}_2(\xi,\eta)$ surface (•), optimized Gumbel logistic $\mathcal{G}_2(\xi,\eta)$ (∘) and optimized Asymmetric logistic $\mathcal{A}_2(\xi,\eta)$ (—) surfaces. Negative numbers indicate probability levels on a decimal logarithmic scale.** *Right*: **Contour plot of the return periods for optimized Gumbel logistic $\mathcal{G}_2(\xi,\eta)$ (∘) and optimized Asymmetric logistic $\mathcal{A}_2(\xi,\eta)$ (—) surfaces. Boxes indicate return periods in days.**

Fig. 10 Right presents contours with return periods in days, 2, 5 and 365 days respectively per contour line. Return period of the order of years is of practical importance for the design of WFSV. It is known that correlation between heave and pitch motions is an important factor, and it has influence on the shape of bivariate coutour lines.

6 Bivariate integral correction

Apart from the obvious prediction of bivariate contours with a given extreme return period, one could mention another possible use, given high correlation between two studied univariate variables, namely vessel heave and pitch. Indeed Fig. 8 exhibits high cross-correlation between two univariate responses with correlation coefficient R_{corr} = 0.75.

The bivariate correction is based on the ACER methodology. The latter involves both the univariate ACER functions as well as the bivariate ACER functions. The unique feature of the ACER functions is that they provide the possibility to portray the exact extreme value distribution inherent in the data time series, both the univariate as well as the bivariate, see Gaidai et al. (2019a); Gaidai et al. (2019b); Xu et al (2019b); Karpa (2015). For the sake of easy reference, the bivariate ACER methodology has been briefly outlined in the Appendix.

This section presents a statistical bivariate integral correction that is based on the bivariate ACER method coupled with the Gumbel logistic model, see Karpa (2015). Note that this correction is not limited to only extreme value estimates, but it can be applied with appropriate bivariate models for any statistical values of interest, in order to improve their accuracy based on synchronously measured longer, highly correlated data records.

To fix ideas, let $Q(t)$ denote the hawser tension of interest, which has been recorded over a time interval of length $\tilde{T}$. Assuming that $\tilde{T}$ is insufficient for accurately predicting the desired univariate extreme tension level with a target low probability of exceedance for a time period much longer than $\tilde{T}$, e.g. 3 hours during a design sea state. Typically, an estimate of the tension level with a return period of 100 times longer may be desired as a design level. This would be formulated as follows: Let $Y = \max\{Q(t); (t_0,\ t_0 + 3 \text{ hours})$, where t_0 is a suitable reference time. The design return period level η_* then satisfies the equation $\text{Prob}\{Y > \eta_*\} = 10^{-2}$.

Let $X = \max\{P(t); (t_0,\ t_0 + 3 \text{ hours})$, and let $F_{XY}(\xi,\eta) = \text{Prob}(X \le \xi,\ Y \le \eta)$ be the joint bivariate cumulative distribution function (CDF) of (X,Y), and let $F_X(\xi)$ and $F_Y(\eta)$ be the corresponding univariate marginal CDFs for X and Y, respectively. As discussed in the previous section, in this paper it is assumed that the bivariate couple $\big(P(t), Q(t)\big)$ has been observed over a period of time $t \in [0, \tilde{T}]$, where the observation duration $\tilde{T}$ is not long enough for accurately predicting the univariate extreme response levels with a target low probability of interest. Now, consider the case when a 'long' record of $P(t)$ is available over a time $t \in [0, T]$, with $T \gg \tilde{T}$, with a corresponding estimated CDF $F_X^{\text{long}}(\xi)$ of the CDF $F_X(\xi)$, which has a probability density function (PDF) $p_X = F_X'$. Then for any Y- response level of interest η_*, with $\Delta \to 0$,

$$F_Y(\eta_*) = F_{XY}(\infty,\eta) = \int_0^{+\infty} \text{Prob}(Y \le \eta_* | X = \xi)\, p_X(\xi) d\xi =$$

$$\int_0^{+\infty} \frac{\text{Prob}(Y \le \eta_*, X \in [\xi, \xi+\Delta])}{\text{Prob}(X \in [\xi, \xi+\Delta])} p_X(\xi) d\xi = \int_0^{+\infty} F'_{XY,X}(\xi,\eta_*)\, d\xi, \quad \text{(A)}$$

with $F'_{XY,X}(\xi,\eta_*)$ denoting the derivative of $F_{XY}(\xi,\eta_*)$ with respect to ξ.

The following copula model for the bivariate extreme value distribution is referred to as the Gumbel logistic model Karpa (2015)

$$F_{XY}(\xi,\eta) = \exp\left\{-\left[\left(-\ln F_X(\xi)\right)^m + \left(-\ln F_Y(\eta)\right)^m\right]^{1/m}\right\} \quad \text{(B)}$$

This bivariate extreme value model has been verified to be a useful model for practical applications provided the marginal extreme value distributions are estimated using the univariate ACER method instead of standard asymptotic extreme value distributions, see Karpa (2015). If Eq. (4) is differentiated with respect to ξ, and substituted into the integrand of Eq. (A), it is obtained that

$$F'_{XY,X}(\xi,\eta_*) = F_{XY}(\xi,\eta_*)\left[1 + \left(\ln F_Y(\eta_*)/\ln F_X(\xi)\right)^m\right]^{\frac{1}{m}-1} \frac{d}{d\xi} \ln F_X(\xi) \quad \text{(C)}$$

The numerical estimate $\hat{F}_Y(\eta_*)$ of $F_Y(\eta_*)$ based on the available time series of recorded data, is obtained by using the following expression,

$$\hat{F}_Y(\eta_*) = \int_0^{+\infty} \hat{F}_{XY}(\xi,\eta_*)\left[1 + \left(\ln \hat{F}_Y(\eta_*)/\ln \hat{F}_X^{long}(\xi)\right)^m\right]^{\frac{1}{m}-1} \frac{d}{d\xi} \ln \hat{F}_X^{long}(\xi)\, d\xi \quad \text{(D)}$$

By applying suggested bivariate correction, the accuracy of extreme response prediction was greatly improved, as discussed here under.

The "long" 3-hour record was chosen as the reference; then the relative ratio of the prediction based on the "short" 0.3 hours observation x_{short} has been divided by the prediction x_{long} based on longer 3 hours observation. The results are summarized in the following table.

Table 3 Bivariate correction results (long term analysis).

	heave	pitch
$x_{\text{short}}/x_{\text{long}}$	0.81	0.80
$x_{\text{corrected}}/x_{\text{long}}$	1.05	1.06

Table 3 shows that there is a practical advantage in applying the bivariate correction introduced in this paper, as it brings shorter prediction quite close to the longer prediction, thus greatly improving accuracy of the extreme value prediction. Note that as mentioned above, a high correlation between two processes is the key requirement for the described correction in order to achieve improved prediction accuracy.

7 Conclusions

This paper presents a study of the combined motion statistics of a wind farm support vessel, during fender docking against a wind tower in actual random seas.

The state-of-art bivariate ACER method has been described and applied to study the vessel coupled motions, specifically heave and pitch, simulated synchronously in time. Low probabilities (high quantiles) contours for the bivariate extreme value distribution have been obtained by adopting bivariate copula models.

When it comes to safety and reliability of WFSV operations, the mulivariate analysis is a more appropriate approach, than the typically used univariate aproach. The presented methodology has the following important advantages:

- Unlike IRORM or SORM, the ACER2D do not simplify non-linearities, inherent in the model.
- Any kind of coupled data can be analysed: either measured or obtained by Monte Carlo simulation.
- Non-stationary data can be analysed.

- Unlike asymptotically based methods (Gumbel, Pareto, Weibull, Peak over threshold etc.) the presented method can accommodate pre-asymptotic behaviour, which means that the data set can be analysed more accurately and efficiently.
- A bivariate correction can be done based on the bivariate statistical analysis for two highly correlated variables. The latter can have practical applications at the design stage.

It should be acknowledged that in order to deliver solid and reliable design analysis for industrial operational purposes, one has to conduct physical tests, and validate numerical simulation results versus experimental. This paper however has been focused on developing an efficient statistical methodology, rather than on hydrodynamic and structural interaction aspects.

8 Appendix: bivariate ACER2D method (in brief)

This paper analyzes bivariate random process $Z(t) = (X(t), Y(t))$, consisting of two scalar component processes $X(t), Y(t)$, measured or simulated synchronously, over certain period of time $(0, T)$. It is assumed that samples $(X_1, Y_1), \dots, (X_N, Y_N)$ are recorded at N time equidistant discrete instants $t_1, \dots, t_N$ within $(0, T)$. Note that the latter assumption of equidistant time sampling surves convenience purpose and does not limit the described methodology.

This Appendix studies the joint cumulative distribution function (CDF) $P(\xi, \eta) := \text{Prob}\left(\hat{X}_N \le \xi, \hat{Y}_N \le \eta\right)$ of the maxima vector $\left(\hat{X}_N, \hat{Y}_N\right)$, with $\hat{X}_N = \max\{X_j ; j = 1, \dots, N\}$, and $\hat{Y}_N = \max\{Y_j ; j = 1, \dots, N\}$. In this paper ξ and η are the heave and pitch angle correspondingly, recorded synchronously at the vessel COG.

Following non-exceedance event is defined $\mathcal{C}_{kj}(\xi, \eta) := \{X_{j-1} \le \xi, Y_{j-1} \le \eta, \dots, X_{j-k+1} \le \xi, Y_{j-k+1} \le \eta\}$ for $1 \le k \le j \le N + 1$. According to the definition of CDF $P(\xi, \eta)$

$$\begin{aligned} P(\xi, \eta) &= \text{Prob}\left(\mathcal{C}_{N+1,N+1}(\xi, \eta)\right) \\ &= \text{Prob}\left(X_N \le \xi, Y_N \le \eta \mid \mathcal{C}_{NN}(\xi, \eta)\right) \cdot \text{Prob}\left(\mathcal{C}_{NN}(\xi, \eta)\right) \\ &= \prod_{j=2}^{N} \text{Prob}\left(X_j \le \xi, Y_j \le \eta \mid \mathcal{C}_{jj}(\xi, \eta)\right) \cdot \text{Prob}\left(\mathcal{C}_{22}(\xi, \eta)\right) \end{aligned} \tag{1}$$

The target CDF $P(\xi, \eta)$ can be reprrsented as in Naess and Karpa (2015); Karpa and Naess (2015); Gaidai et al. (2016)

$$P(\xi, \eta) \approx \exp\left\{-\sum_{j=k}^{N} \left(\alpha_{kj}(\xi; \eta) + \beta_{kj}(\eta; \xi) - \gamma_{kj}(\xi, \eta)\right)\right\};\ \xi, \eta \to \infty \tag{2}$$

for sufficiently the large conditioning order parameter k with $\alpha_{kj}(\xi; \eta) := \text{Prob}\left(X_j > \xi \mid \mathcal{C}_{kj}(\xi, \eta)\right), \beta_{kj}(\eta; \xi) := \text{Prob}\left(Y_j > \eta \mid \mathcal{C}_{kj}(\xi, \eta)\right), \gamma_{kj}(\xi, \eta) := \text{Prob}\left(X_j > \xi, Y_j > \eta \mid \mathcal{C}_{kj}(\xi, \eta)\right)$.

From Eq. (2) shows that accurate estimate of the bivariate CDF $P(\xi, \eta)$ requires accurate estimate of functions $\{(\alpha_{kj}(\xi; \eta) + \beta_{kj}(\eta; \xi) - \gamma_{kj}(\xi, \eta))\}_{j=k}^{N}$. Let one intdoduce k-th order bivariate average conditional exceedance rate (ACER2D) functions

$$\mathcal{E}_k(\xi, \eta) = \frac{1}{N - k + 1} \sum_{j=k}^{N} \left(\alpha_{kj}(\xi; \eta) + \beta_{kj}(\eta; \xi) - \gamma_{kj}(\xi, \eta)\right), \quad k = 1, 2, \dots \tag{3}$$

Then, when $N \gg k$, one has

$$P(\xi, \eta) \approx \exp\{-(N - k + 1)\, \mathcal{E}_k(\xi, \eta)\};\ \xi, \eta \to \infty \tag{4}$$

Estimation of bivariate ACER2D functions $\mathcal{E}_k(\xi, \eta)$ for the simulated/observed stationary/non-stationary time series constitutes counting of exceedance events. For the detailed estimation of the bivariate ACER2D functions, see Naess and Karpa (2015); Karpa and Naess (2015); Gaidai et al. (2016).

In the above, no assumption about stationarity has been made. Hence, it also applies to long term time series. However, in this case it is often expedient to reformulate the expressions. Given the scatter diagram consisting of $m = 1, .., M$ sea states (long term statistics), each sea state having an individual probability p_m, with the obvious equality $\sum_{m=1}^{M} p_m = 1$. Then it is natural to rewrite the ACER2D function definition as follows $\mathcal{E}_k(\xi, \eta) = \sum_{m=1}^{M} \mathcal{E}_k(\xi, \eta, m)\, p_m$, with $\mathcal{E}_k(\xi, \eta, m)$ being the ACER2D function estimated for an individual m-th stationary sea state. This provides a practical expression for the long term ACER2D function.

For any couple of random variables (X, Y) with marginal CDFs $F_x(\xi)$ and $G_y(\eta)$, the joint CDF $H_{xy}(\xi,\eta) = \text{Prob}\,(X \le \xi, Y \le \eta)$ can be represented by the bivariate copula $C(u,v)$ as $H_{xy}(\xi,\eta) = C(F_x(\xi),\ G_y(\eta))$, cf. e.g. Balakrishnan and Lai (2009); Sklar (1959); Nelsen (2006); Yue et al. (1999); Yue and Wang (2004); Hougaard (1986); Tiago de Oliveira (1984). The latter is a general theoretical result that holds for any bivariate extreme value distribution.

In this paper two types of Pickands dependence function have been applied: The optimized Gumbel logistic (GL) Gumbel (1960a); Gumbel (1960b); Gumbel (1961) and the optimized Asymmetric logistic (AL), Coles and Tawn (1991); Coles and Tawn (1994); Coles (2001); Tawn (1988); Balakrishnan and Lai (2009); Sklar (1959); Nelsen (2006); Pickands (1981); Gudendorf and Segers (2010).

It is now assumed that the marginal extreme value distributions (EVD) are represented by the univariate ACER functions, see Naess and Karpa (2015); Karpa and Naess (2015); Gaidai et al. (2016)

$$\begin{aligned} F_x(\xi) &\approx \exp\{-(N-k+1)\varepsilon_k^x(\xi)\}, \qquad \xi \ge \xi_1 \\ G_y(\eta) &\approx \exp\{-(N-k+1)\varepsilon_k^y(\eta)\}, \qquad \eta \ge \eta_1 \end{aligned} \tag{5}$$

with $\varepsilon_k^x(\xi) = q_k^x \exp\{-a_k^x(\xi - b_k^x)^{c_k^x}\}$ and similar definition for $\varepsilon_k^y(\eta)$.

The detailed optimization procedure for estimation of parameters $a_k^x, b_k^x, c_k^x, q_k^x, a_k^y, b_k^y, c_k^y, q_k^y$ is outlined in Naess and Karpa (2015); Karpa and Naess (2015); Gaidai et al. (2016).

The choice of copula model is now determined by the accuracy obtained by fitting $H_{xy}(\xi,\eta)$ to the empirical $P(\xi,\eta)$.

References

Bondarenko, O. (2015), "The Statistical Analysis of Principal Particulars of Wind Farm Support Vessels", Second Design & Operation of offshore Wind Farm Vessels conference, Royal Institution of Naval Architects, London.

Wu, M. K. (2014), "Numerical analysis of docking operation between service vessels and offshore wind turbines", Ocean Engineering, Vol. 91, pp. 379-388.

Zhang, P., Dai, L., Liu, Y., (2014a), "Modelling Operation of Service Vessels in Offshore Wind Farms Using Stochastic Activity Networks", Ship Technology Research, Vol. 61(1), 48-58, DOI: 10.1179/str.2014.61.1.004

Naess, A, and Moan, T. (2013), "Stochastic dynamics of marine structures", Cambridge University Press.

Price, W.G., and Bishop, R.E.D. (1974), "Probabilistic theory of ship dynamics", Chapman and Hall, London.

Sandvik, P.C. (2010), "Docking application and significant waves - simulation of dynamic behavior during docking for personnel transfer", Kockum Workshop on service vessels for personnel transportation to offshore wind turbines, Karlskrona, Sweden.

Zhang, L, and Zhu, R, and Niu, F. (2014b), "Offshore wind power operational ship design analysis", Journal International offshore wind, Vol. 6, pp. 62-66.

Phillips, S, and Shin, I, and Armstrong, C. (2014), "Performance evaluation of wind-farm support vessels", Design & Operation of Wind Farm Support Vessels, London, UK.

Phillips, S, and Shin, I, and Armstrong, C. (2015), "Crew transfer vessel performance evaluation", Design & Operation of Wind Farm Support Vessels, London, UK.

Naess, A, and Karpa, O. (2015), "Statistics of bivariate extreme wind speeds by the ACER2D method", J. Wind Eng. and Ind. Aerodyn. Vol 139, pp.82–88.

Karpa, O., and Naess, A. (2015), "Statistics of Extreme Wind Speeds and Wave Heights by the Bivariate ACER2D Method", J. Offshore Mech. and Arctic Eng., 137(2).

Gaidai, O, and Storhaug, G, and Naess, A. (2016), "Extreme large cargo ship panel stresses by bivariate ACER2D method", Vol. 127, pp. 368-386.

Heffernan, J.E., and Tawn, J.A. (2004), "A Conditional Approach for Multivariate Extreme Values", Journal of the Royal Statistic Society: Series B, 66(3), pp. 497－546.

Ewans, K. (2014), "Evaluating Environmental Joint Extremes for the Offshore Industry Using the Conditional Extremes Model", Journal of Marine Systems, 130, pp. 124-130.

Zhao, Y.G., and Ono, T. (1999), "A general procedure for first/second order reliability method (FORM/SORM)", Structural safety 21(2), pp. 95-112.

http://www.globalwavestatisticsonline.com/

DNV-RP-H103, (2011), "Modelling and analysis of marine operations".

DNV-RP-C205, (2010), "Environmental conditions and environmental loads".

Wang, Z., and Wu, K., and Zhou, L., and Wu, L., (2012), "Wave characteristics and extreme parameters in the Bohai sea", China Ocean Engineering, Vol. 26(2), pp. 341- 350.

Gumbel, E. J. (1960a), "Multivariate Extremal Distributions", Bull. l'Institut Int. Stat., 37(2), pp. 471–475.

Gumbel, E. J. (1960b), "Bivariate Exponential Distributions", J. Am. Stat. Assoc., 55(292), pp. 698–707.

Gumbel, E. J. (1961), "Bivariate Logistic Distributions", J. Am. Stat. Assoc., 56(294), pp. 335–349.

Gumbel, E. J., and Mustafi, C. K. (1967), "Some Analytical Properties of Bivariate Extremal Distributions", J. Am. Stat. Assoc., 62(318), pp. 569–588.

Coles, S. G., and Tawn, J. A. (1991), "Modeling Extreme Multivariate Events", J. R. Stat. Soc. B, 53(2), pp. 377–392.

Coles, S. G., and Tawn, J. A. (1994), "Statistical Methods for Multivariate Extremes: An Application to Structural Design", J. R. Stat. Soc. C, 43(1), pp. 1–48.

Coles, S. (2001), "An Introduction to Statistical Modeling of Extreme Values", Springer Series in Statistics, Springer-Verlag, London, UK.

Tawn, J. A. (1988), "Bivariate Extreme Value Theory: Models and Estimation", Biometrika, 75(3), pp. 397–415.

Balakrishnan, N., and Lai, C.D. (2009), "Continuous Bivariate Distributions", Springer Science Business Media, New York.

Sklar, M. (1959), "Fonctions de repartition dimensions et leurs marges", Publications of the Institute of Statistics of the University of Paris, Paris, France, Vol. 8, pp. 229–231.

Nelsen, R. B. (2006), "An Introduction to Copulas (Springer Series in Statistics) ", Springer Science Business Media, New York.

Pickands, J. (1981), "Multivariate Extreme Value Distributions", Proceedings of the 43rd Session of the International Statistical Institute, Bulletin of the International Statistical Institute, Vol. 49, pp. 859–878.

Gudendorf, G., and Segers, J. (2010), "Extreme-Value Copulas", Copula Theory and Its Applications, Springer-Verlag, Berlin, Germany, Chap. 6.

Yue, S., and Ouarda, T., and Bobee, B., and Legendre, P., and Bruneau, P. (1999), "The Gumbel Mixed Model for Flood Frequency Analysis", J. Hydrol., 226(1–2), pp. 88–100.

Yue, S., and Wang, C. Y. (2004), "A Comparison of Two Bivariate Extreme Value Distributions", Stochastic

Environ. Res. Risk Assessment, 18(2), pp. 61–66.

Hougaard, P. (1986), "A Class of Multivariate Failure Time Distributions", Biometrika, 73(3), pp. 671–678.

Tiago de Oliveira, J. (1984), "Bivariate Models for Extremes; Statistical Decision", Statistical Extremes and Applications, Springer, New York, pp. 131–153.

AQWA users manual, (2013), Release 15.0, ANSYS, Inc.

AQWA theory manual, (2013), Release 15.0, ANSYS, Inc.

Karpa, O., 2015, "Development of bivariate extreme value distributions for applications in marine technology", Marine Technology, NTNU, Trondheim.

Lv, X., Yuan, D., Ma, X., Tao, J., 2014. Wave characteristics analysis in Bohai Sea based on ECMWF wind field. Ocean Engineering, Vol 91, pp. 159-171.

Zhang, J., Gaidai, O., Gao, J., (2018). "Bivariate extreme value statistics of offshore jacket support stresses in Bohai bay", J. Offshore Mech. Arctic Eng. 140 (4), 041305. https://doi.org/10.1115/1.4039564.

Reed, A.M. and Beck, R.F. (2016). "Advances in the Predictive Capability for Ship Dynamics in Extreme Waves", SNAME Transactions, Vol. 124.

Xu, X., Sahoo, P., Evans, J., and Tao, Y., (2019a), "Hydrodynamic performances of FPSO and shuttle tanker during side-by-side offloading operation, ships and offshore structures", https://doi.org/10.1080/17445302.2019.1580845.

Xu, X., Gaidai, O., Naess, A., Sahoo, P., (2019b), "Improving the prediction of extreme FPSO hawser tension, using another highly correlated hawser tension with a longer time record", Applied Ocean Research, Vol. 88, pp. 89–98.

DNV-RP-H103, (2011). Modelling and analysis of marine operations.

Naess, A., Gaidai, O., and Haver, S., 2007. "Estimating extreme response of drag dominated offshore structures from simulated time series of structural response". Ocean Engineering, Vol 34, pp. 2188-2197.

Gaidai, O., Naess, A., Karpa, O., Xu, X., Cheng, Y., Ye, R. (2019a), "Improving extreme wind speed prediction for North Sea offshore oil and gas fields", Applied Ocean Research, Vol 88, pp. 63–70.

Gaidai, O., Naess, A., Xu, X, Cheng, Y, (2019). "Improving extreme wind speed prediction based on a short data sample, using a highly correlated long data sample", Journal of Wind Engineering & Industrial Aerodynamics, Vol 188, pp. 102–109.